

MALAYSIAN JOURNAL OF ANALYTICAL SCIENCES



Journal homepage: https://mjas.analis.com.my/

Research Article

Magnetic iron oxide for the removal of Allura red and Erioglaucine A dyes: Synthesis and adsorption optimization

Nurul Yani Rahim¹, Siti Hajar Abdullah¹, Nurina Izzah Mohd Husani², Nor Munira Hashim², Nur Hidayah Sazali³, and Nur Nadhirah Mohamad Zain^{2*}

Received: 25 April 2025; Revised: 29 September 2025; Accepted: 6 October 2025; Published: 26 October 2025

Abstract

The environmental hazards associated with the introduction of synthetic colorants into aquatic systems are substantial, as they can be detrimental to both aquatic organisms and humans, as a result of inadequate disposal management. The co-precipitation method was employed to synthesize Fe₃O₄ magnetic nanoparticles, with ferrous chloride tetrahydrate (FeCl₂·4H₂O) and ferric chloride hexahydrate (FeCl₃ 6H₂O) serving as the starting materials. The nanoparticles that were synthesized underwent a thorough characterization. X-ray Diffraction (XRD) analysis revealed distinct diffraction peaks at $2\theta = 30.20^{\circ}, 35.55^{\circ}, 43.35^{\circ}$, 57.20°, and 63.10°, which are associated with the cubic spinel structure of Fe₃O₄, thus confirming the material's crystallinity. Ultra-High-Resolution Scanning Electron Microscopy (UHR-SEM) micrographs displayed spherical, agglomerated morphologies within the 300-500 nm range. Brunauer-Emmett-Teller (BET) analysis indicated a mesoporous structure characterized by a specific surface area of 58.62 m²/g. Concurrently, Vibrating Sample Magnetometry (VSM) measurements exhibited pronounced magnetic behavior, with a saturation magnetization (Ms) of 86.83 emu/g, confirming the presence of superparamagnetism. The adsorption performance of Fe₃O₄ nanoparticles for Allura Red and Erioglaucine A was systematically evaluated using the Taguchi design approach. This evaluation was carried out under varying pH, adsorbent mass, and sample volume conditions, while parameters including temperature, contact time, and initial concentration were analyzed independently. The results indicated a monolayer adsorption process driven by chemisorption, with kinetics conforming to a pseudo-second-order model, and equilibrium data aligning with the Langmuir isotherm (R² = 1). The thermodynamic analysis confirmed that the adsorption process is exothermic. In practical applications, when using Fe₃O₄ nanoparticles on real wastewater samples, a high removal efficiency for Allura Red was observed, ranging from 94.57% to 100.13%, with a relative standard deviation (%RSD) of less than 1.40%. The removal efficiency for Erioglaucine A exhibited significant variability, ranging from 1.19% to 100.08%, with a %RSD of less than 20.00%. This variability likely arises from limitations in equilibrium diffusion at higher dye concentrations and differences in dye molecule structures. Overall, the results indicated that Fe₃O₄ nanoparticles demonstrated significant efficacy in the magnetic separation and elimination of Allura Red. However, optimization strategies may be necessary to improve the removal of Erioglaucine A in complex wastewater matrices.

Keywords: Magnetic nanoparticles, Allura red, Erioglaucine A, Taguchi design method, adsorption

Introduction

Synthetic dyes play a crucial role in various industries, including textiles, food processing, paper, leather, and paints, primarily due to their vibrant hues, chemical stability, and production cost-effectiveness. [1,2,3]. However, the effluents containing these dyes pose significant environmental challenges, with over 100,000 dyes commercially available and global production exceeding 700,000 tonnes annually. An

estimated 15% of these dyes are lost during processing and released into the environment, raising concerns due to their non-biodegradable, toxic, mutagenic, and carcinogenic properties [4, 5]. Such contamination adversely affects aquatic ecosystems and human health by reducing light penetration, altering dissolved oxygen levels, and increasing biological and chemical oxygen demand. Traditional treatment methods like coagulation, flocculation, photocatalysis, and

¹School of Chemical Science, Universiti Sains Malaysia, 11800 Pulau Pinang, Malaysia

²Department of Toxicology, Advanced Medical and Dental Institute, Universiti Sains Malaysia, 13200 Kepala Batas, Penang, Malaysia

³Institute of Sustainable Energy & Resources, Universiti Teknologi PETRONAS, 32610 Seri Iskandar, Perak, Malaysia

^{*}Corresponding author: nurnadhirah@usm.my

membrane filtration have limitations, including high operational costs, the generation of secondary sludge, and issues with membrane fouling [1,6]. In contrast, adsorption has emerged as an efficient and cost-effective technique for dye removal. Its simplicity and effectiveness across various conditions enable it to address low and high contaminant concentrations [7].

Among the materials used for adsorption, magnetic Fe₃O₄ nanoparticles have gained attention due to their elevated surface area, availability of reactive sites, and superparamagnetic properties, allowing easy recovery from aqueous solutions using external magnetic fields [6,7,8]. The environmentally sustainable synthesis of these nanoparticles through a co-precipitation method further position them as suitable candidates for largescale applications. Nevertheless, there is still a limited understanding of the adsorption behavior of commonly used food dyes, such as Allura Red and Erioglaucine A. particularly regarding mechanisms involved. thermodynamic considerations, and the parameters influencing the process.

This study employs Taguchi optimization, a statistical design of experiments approach, to systematically investigate and enhance key factors such as pH, adsorbent dosage, and sample volume. This methodology effectively reduces the number of experimental trials while identifying the critical parameters influencing dye removal efficiency [9,10]. Additionally, comprehensive adsorption kinetics, isotherm modeling, and thermodynamic analyses are conducted to thoroughly understand the adsorption mechanisms. Kinetic modeling aims to pinpoint the rate-controlling steps, isotherm models characterize the interactions between the dye and the adsorbent surface, and thermodynamic analysis evaluates the feasibility, spontaneity, and energetic aspects of the adsorption process [11,12].

The primary objective of this study is to synthesize Fe_3O_4 nanoparticles using a co-precipitation method and to evaluate their adsorption efficiency for Allura Red and Erioglaucine A under optimized conditions. By integrating Taguchi optimization with adsorption modeling, this research aims to enhance the understanding of Fe_3O_4 —dye interactions and to contribute to the development of cost-effective, sustainable, and magnetically recoverable adsorbents for wastewater treatment applications.

Materials and Methods Chemicals and reagents

In this research, the chemicals that have been used are ferrous chloride tetrahydrate (FeCl₂.4H₂O) (98%) and ferric chloride hexahydrate (FeCl₃.6H₂O) (\geq 98%)

from Chemiz Malaysia (Shah Alam, Selangor) and Merck (Darmstadt, Germany), respectively were used to synthesize the MNPs, Fe₃O₄. Methanol (HPLC grade) was supplied by Chemiz Malaysia (Shah Alam, Selangor), and ammonia solution (NH₃) (28%) utilized was from QReC Chemicals (New Zealand). Dyes, such as Allura red (80%) and Erioglaucine A (>99%) powders, were purchased from R&M Marketing (Essex, U.K.). No additional purification was performed on the reagents and chemicals before

Synthesis of Fe₃O₄ adsorbent

In this experiment, Fe₃O₄ was prepared using a conventional co-precipitation method with slight modification [15]. About 1.13 g FeCl₂.4H₂O and 3.03 g FeCl₃.6H₂O were mixed and dissolved in 50 mL of deionized water. The mixture was then stirred under nitrogen gas at 400 rpm, 50°C for 30 min. 12 mL 28% ammonia solution was added into the mixture solution to allow the magnetization process and agitated for an hour at 90°C under nitrogen gas before collecting the final products using an external magnet. Then, the materials were washed using 50 mL of methanol and 50 mL of deionized water alternately several times. After that, the products were dried in an oven overnight. Lastly, the dried products were crushed and ground using a pestle and mortar, before being stored for further use.

Instrumentation

The studies were conducted using deionized water obtained from the Sartorius Stedim deionized water dispenser, Milli–Q® system (Arium 611 DI). A pH meter (BP3001 Trans Instruments) was utilized to measure and adjust the pH value. The initial and final concentrations of these dyes were determined by a UV-vis spectrophotometer (Perkin Elmer Lambda25) with a 1 cm quartz cell, where the λ_{max} for Allura Red was 504.2 nm, and the λ_{max} for Erioglaucine A was 629.1 nm. An incubator shaker (IKA, KS4000 control) was used to shake the sample solution at 200 rpm with adjustable temperature and time. In contrast, a mechanical shaker (Orbitron) was used to shake the solution at a similar speed and at room temperature with adjustable time.

Characterization of the synthesized Fe₃O₄ adsorbent

The surface morphology and structural characteristics of the Fe₃O₄ adsorbent were assessed using Ultra High-Resolution Scanning Electron Microscopy (UHR-SEM) (QUANTA FEG650, Hillsboro, Oregon, USA) at magnifications ranging from 3000× to 150,000×. Crystallographic parameters, including phase composition, unit cell dimensions, and lattice configurations, were determined using X-ray

diffraction (XRD) (Siemens D5000, Frimley, UK). XRD measurements utilized Cu K α radiation (λ = 1.5418 Å) at a scanning rate of 0.02 s⁻¹ across a 2 θ range of 10–70°, with an operating voltage of 40 kV and a current of 100 mA.

Brunauer-Emmett-Teller (BET) from Micromeritics Tristar II-Mesopore model (USA) was used to determine the gas particle's physical adsorption on a solid surface and the adsorbent's surface area. Before analysis, the sample was degassed at 80°C for 2 hours to eliminate the moisture content. A vibrating sample magnetometer (VSM) measures the strength of a sample's magnetic field and evaluates how well the sample can couple with an external magnetic field. The sample's magnetic property was analyzed under room temperature using the Lake Shore 7404 series VSM (McCourkle Boulevard, WO, USA).

Batch adsorption study

The Fe₃O₄ particles were employed as adsorbents for the removal of both dyes. The adsorption process was systematically investigated using the Taguchi design and the One-Variable-at-a-Time (OVAT) method. The Taguchi design facilitated the assessment of key factors such as solution pH, adsorbent dosage, and sample volume. At the same time, the OVAT method was used to explore the effects of adsorption time, initial dye concentration, and temperature. Batch adsorption studies were conducted to evaluate the removal efficiency of Allura Red and Erioglaucine A on Fe₃O₄. The Taguchi Orthogonal Array (OA) design, a fractional factorial method developed by Dr. Genichi Taguchi [16], was employed to identify an optimized subset of factor-level combinations. The experimental design is summarized in Table 1, which details three factors at four levels, utilizing a standard L16 orthogonal array that comprises 12 experimental trials.

In this study, the objective is to optimize the removal percentage of both dyes on magnetic nanoparticles, utilizing the larger-the-better (LTB) type of robustness criterion, as Genichi Taguchi classified the signal-to-noise (S/N) ratio into three objectives: larger-the-better (LTB), smaller-the-better (STB), and

nominal-the-best (NTB). The S/N ratio measures the relationship between the mean percent of the removal (signal) and the standard deviation (noise), indicating the impact of noise factors on performance. Therefore, the target property, percentage recovery, which should be maximized, aligns with the larger-the-better (LTB) optimization criterion.[16]. The relationship between the S/N ratio and the removal percentage is defined using specific equations. (1) – (4):

$$\frac{s}{N} = -10\log\left(\frac{1}{n}\sum_{i=1}^{n}\frac{1}{y_i^2}\right)$$
 (Eq. 1)

Where y_i is the average percentage recovery for n repetitions. The analysis of the mean (ANOM) determines the effect of a variable level on the S/N ratio, to measure the deviation caused by the overall mean of the signal.

Meanwhile, the analysis of variance (ANOVA) of S/N ratios is used to obtain the relative effect of the variables. The computation of the values for ANOM and ANOVA is based on the following equation:

$$m_i = \left(\frac{1}{N_1}\right) \sum_{i=1}^4 \left(\frac{s}{N}\right) i$$
 (Eq. 2)

Where N_1 is the number of levels for each variable and m_i is the mean of S/N for each level. The sum of squares (SS) for each variable is calculated according to the following equation:

Sum of square (SS) =
$$\sum_{i=1}^{5} N_1 (m_i - \bar{m}_i)^2$$
 (Eq. 3)

Where \overline{m}_i is the contribution of each variable level to the S/N ratio and m_i is the mean of m_i for a specified variable. The relative importance of various experimental variables (factor effect) is calculated using the following equation:

Factor effect =
$$\frac{SS}{D_f \times \sum \frac{SS}{D_f}}$$
 (Eq. 4)

Where D_f is the number of the variable level minus 1.

Table 1. Variables and designs of experiments using the Taguchi Method

No.	Parameter		Level/Value		
		1	2	3	4
1	рН	2	3	4	5
2	Fe ₃ O ₄ amount (mg)	5	10	15	20
3	Sample volume(mL)	5	10	15	20

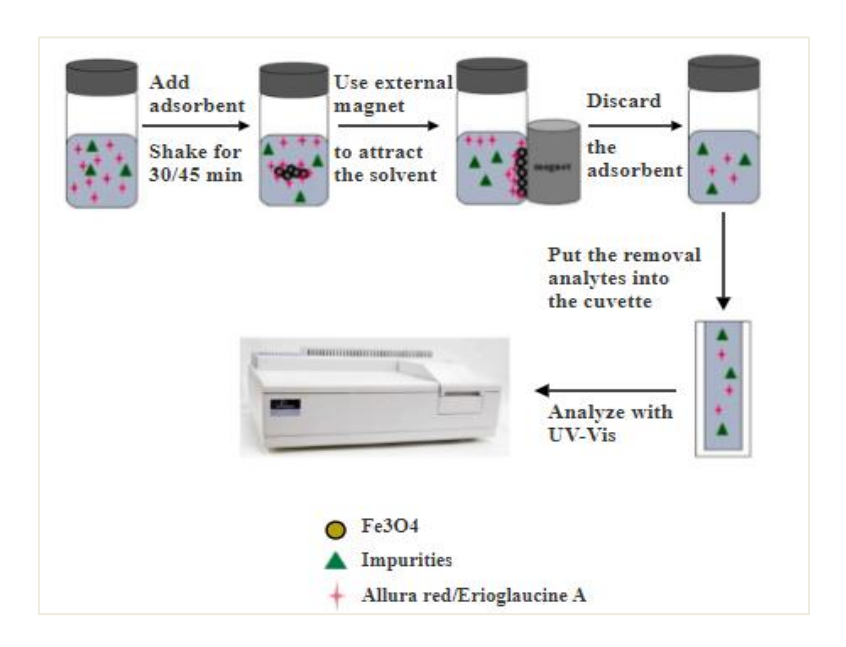


Figure 1. Adsorption of Allura red/Erioglaucine A from the dye solution

Based on the results from the design proposed, batch experiments were carried out to investigate the adsorption of both dyes on Fe₃O₄ particles. In this adsorption study, about 10 mg of Fe₃O₄ was placed in a closed 20 mL vial containing 10 mg/mL (Allura Red or Erioglaucine A). The solutions were shaken at 200 rpm for 45 min (Allura Red) and 30 min (Erioglaucine A) under room temperature to ensure the adsorption between Allura Red or Erioglaucine A molecules and the Fe₃O₄ adsorbent's active site occurs. An external magnet was used to isolate the adsorbent from the dye solution after the process, as illustrated in **Figure 1**.

The effects of different pH (2-5) were investigated using 0.1 M NaOH and 0.1 M HCl, contact time (5-45 min), the mass of the adsorbent (5-20 mg), initial concentration (5-40 mg/L), and temperature (298-333 K). The residual concentration was analyzed using UV-vis spectrophotometry. The removal percentage (R%) and adsorption capacity (mg/g) are calculated using Equation (5) and Equation (6), respectively:

$$R\% = \frac{c_0 - c_e}{c_0} \times 100$$
 (Eq. 5)

$$q_e = \frac{c_0 - c_e}{W} \times V \tag{Eq. 6}$$

Where C_0 (mg/L) and C_e (mg/L) are the initial and equilibrium concentrations of the solutions. W (g) is the mass of the adsorbent used, while V (L) is the volume of the solution.

Pre-treatment of real samples

Three different food industrial wastewater samples were collected randomly from various places in an industrial area in Pulau Pinang, Malaysia. All samples were filtered using a vacuum filter and stored in appropriate containers before use.

Thermodynamic study

Thermodynamic parameters were assessed to analyse the feasibility and characteristics of dye adsorption. The changes in Gibbs free energy (ΔG°), enthalpy (ΔH°), and entropy (ΔS°) were determined using the following equations (7) and (8):

$$\Delta G^{\circ} = -RT \ln K_{d}$$
 (Eq. 7)

$$lnK_{d} = \frac{\Delta S^{\circ}}{R} - \frac{\Delta H^{\circ}}{RT}$$
 (Eq. 8)

where R, is the gas constant (8.314 kJmol $^{-1}$ K $^{-1}$), T is the temperature in Kelvin, and K_d indicates the equilibrium constant.

The value of ΔG° values confirms the spontaneity of adsorption, while the ΔH° indicates exothermic or endothermic behaviour. The value of ΔS° indicates the randomness at the solid–liquid interface [15, 16].

Kinetic study

The adsorption kinetics of Allura Red and Erioglaucine A onto Fe₃O₄ nanoparticles were analyzed using five models: pseudo-first-order, pseudo-second-order, intraparticle diffusion, external diffusion, and Elovich. The governing equations are:

Pseudo-first order in the kinetics was proposed by Lagergren in 1998. This model describes the adsorption of the materials to turn the aqueous solution into many types of solid materials. Equation (9) was proposed as:

$$\frac{dq_t}{d_t} = k_1(q_{e-}q_t) \tag{Eq. 9}$$

At t=0 and $q_t=0$, Equation (10) will be:

$$\log(q_e - q_t) = \log q_e - \frac{k_1}{2303}t$$
 (Eq. 10)

Where q_e (mg/g) is the capacity of the dye to adsorb at equilibrium, q_t (mg/g) is the capacity of the dye to adsorb at a given time, and k_1 is the rate constant.

Pseudo-second order model's Equation (11) was given as:

$$\frac{t}{q_t} = \frac{1}{q_e}t + \frac{1}{\kappa_2 q_e^2}$$
 (Eq. 11)

Where the contact time is noted as t, and K_2 is the rate constant. These values can be obtained from the graph plotted. The graph plotted between $(1/q_t)$ against t produces a straight line with the intercept and slope at $1/q_c$ and $1/K_2q_c^2$

Intraparticle diffusion was used to evaluate the rate of diffusion at the early step of the adsorption process. This model can be expressed by Equation (12):

$$q_t = K_t^{1/2} + c$$
 (Eq. 12)

Where K is the rate constant, t is the time, and c is the intercept. In intraparticle diffusion, the rate constant is directly proportional to the layer thickness at the boundary.

Meanwhile, the external diffusion was calculated using Equation (13):

$$ln\frac{c_t}{c_0} = -k_{ext}t (Eq. 13)$$

Where k_{ext} is the rate of the diffusion parameter, C_0 is the initial analyte concentration, and C_t is the concentration of solute in the liquid at a given time.

The Elovich kinetic model could be evaluated by the given Equation (14):

$$q_t = \frac{1}{\beta}(\ln \alpha \beta) + \frac{1}{\beta}\ln t$$
 (Eq. 14)

where α stands for the initial rate of sorption, β the activation energy, and the binding capacity is q_t

Isotherm study

Referring to the study by Sumanjit et. al. [14], to describe equilibrium adsorption behavior, five isotherm models, including Langmuir, Freundlich, Temkin, Dubinin–Radushkevich (D–R), and Halsey, were applied. The Langmuir Equation (15) was proposed as follows:

$$q_e = \frac{q_m R_L C_e}{R_L C_e + 1}$$
 (Eq. 15)

Where q_m is the adsorption capacity in mg/g, b is the sorption energy in L/mg to the equilibrium of concentration of the analyte, C_e in mg/L. By plotting the graph C_e/q_e versus C_e , the values of q_m and b can be obtained. The slope and intercept can be obtained based on the straight line. The important properties of the Langmuir isotherm model can be proposed in a factor called the dimensionless constant separation factor, R_L in Equation (16):

$$R_{L=}\frac{1}{1+K_LC_0}$$
 (Eq. 16)

Where C_0 represented the initial concentration of the solute in mg/L. If the calculated R_L value was less than unity, it showed the favourable uptake of the sorbent.

Freundlich isotherm was employed to describe the heterogeneous system. This isotherm is also applied to plot the equilibrium data of the adsorption. Equation (17) is used for this isotherm is below:

$$\log \frac{x}{m} = \log Kf + \frac{1}{n \log Ce}$$
 (Eq. 17)

Where x is the amount of dye adsorbed (mg), m is the weight of the adsorbent used (g), Ce is the equilibrium concentration of the dye in solution (mg/L), and Kf and n are the Freundlich constants, n is the heterogeneity factor (adsorption intensity), and Kf denotes the adsorption capacity. The values of n > 1 reflect the favourable adsorption conditions.

The Temkin model was proposed based on the electrostatic interaction. Equation (18) is:

$$q_e = \beta ln K_T + \beta ln C_e$$
 (Eq. 18)

Where β is obtained from RT/b_T, KT, the heat adsorption, and the energy of equilibrium binding are related to the Temkin constant, K_T. This model indicates how the adsorption process relates to the adsorbent concentration, which should not be too low or too high. The heat energy will decrease if the adsorbent active site is occupied gradually during the analyte and adsorbent interaction. The Temkin isotherm model states that the adsorbent has uniform energies in all the binding sites [14].

The variation of adsorption energy is described as b_T . If the adsorption reaction was more than 1, it is known as an exothermic reaction; if the value was less than 1, it is an endothermic reaction.

The Hasley isotherm model has described the adsorption on the multilayer [14]. It can be expressed by Equation (19):

$$lnq_e = \left[\frac{1}{n}lnK_H\right] - \frac{1}{n}lnC_e$$
 (Eq. 19)

Method validation and real samples analysis

In order to evaluate the established adsorption study using Fe3O4 adsorbent, related analytical parameters of the method, including the linear range, coefficient of determination, repeatability, and reproducibility, were studied by employing food industrial wastewater samples under optimized experimental conditions.

Linearity

The linearity of the dyes in wastewater samples was evaluated by constructing calibration curves for each analyte. Standard solutions were prepared with concentrations ranging from 10 to 40 mg/L for Allura Red and from 5 to 30 mg/L for Erioglaucine A. Calibration curves were generated by plotting absorbance values (A) against the corresponding analyte concentrations (mg/L). The coefficient of determination (R²) was calculated to assess the linear relationship between concentration and instrument response.

Precision and removal study

The precision of the adsorption studies was evaluated through intra-day (repeatability) and inter-day (reproducibility) tests, which are expressed as the relative standard deviation (%RSD). To assess these parameters, samples of food industrial wastewater were spiked with three different concentrations of Allura Red (10, 25, and 40 mg/L) and Erioglaucine A (5, 15, and 30 mg/L), respectively. These concentration levels were chosen to represent low, medium, and high ranges of the dyes, reflecting concentrations typically found in industrial effluents and aligning with the method's linear dynamic range. Intra-day precision was determined by conducting five replicate measurements within a single day, while inter-day precision was evaluated over three consecutive days. This design ensures a thorough assessment of the method's reliability, demonstrating its consistency under varying operational conditions and its applicability for monitoring dye pollutants in real environmental matrices. The relative standard deviation (RSD) value was calculated using Equation (20) and Equation (21):

$$SD = \sqrt{\frac{\sum (x - \bar{x})^2}{n - 1}}$$
 (Eq. 20)

$$RSD = \frac{SD}{\bar{x}} \times 100$$
 (Eq. 21)

Where \bar{x} represents the mean, x is the result of every run, and n is the number of measurements (repeatability).

The optimized adsorption parameters were then used to analyze real water samples to investigate removal percentage and matrix effects. The food industrial wastewater was spiked at three different concentrations of Allura Red (10, 25, and 40 mg/L) and Erioglaucine A (5, 15, and 30 mg/L). The removal percentage and RSD were calculated based on Equation (5) and Equation (8), respectively.

Regeneration study

The optimum adsorbent amount and contact time conditions were used for this study. After each adsorption was analyzed, the adsorbent was collected and desorbed with methanol HPLC Grade and dried at 60°C for 24 hours. This procedure was repeated until the removal efficiency of the adsorbent was less than 80% for both dyes [14].

Results and Discussion Characterizations of Fe₃O₄ adsorbent UHR SEM analysis

The morphology of the Fe₃O₄ nanoparticles adsorbents was observed using UHR-SEM, as shown in Figure 2. The synthesized Fe₃O₄ nanoparticles displayed a spherical morphology with a uniform size distribution, characterized by roughened surfaces and agglomeration under 150k and 100k magnification. Such spherical morphology is advantageous as it provides a larger number of accessible surface sites, thereby facilitating enhanced interactions with dye molecules during the adsorption process. This observation aligns with previous reports, which have demonstrated that spherical Fe₃O₄ nanoparticles exhibit superior adsorption performance due to their high surface availability and effective surface-active sites [13, 17].

BET analysis

The surface area and pore characteristics of Fe₃O₄ nanoparticles were analyzed through nitrogen adsorption—desorption, as depicted in **Figure 3**. The isotherm reveals a type IV curve with an H3 hysteresis loop, indicating the presence of mesopores [18,19]. The measured BET surface area was 58.62 m²/g. This mesoporous structure enhances adsorption by creating

effective pathways for the diffusion of dye molecules and reducing the risk of pore blockage, particularly for larger organic compounds, such as Allura Red and Erioglaucine A [22]. The combination of mesoporosity and sufficient surface area enhances the efficiency of the adsorbent by providing numerous accessible active sites for pollutant binding.

XRD analysis

The XRD patterns of the synthesized Fe₃O₄ nanoparticles are displayed in Figure 4. The observed diffraction peaks at $2\theta = 30.1^{\circ}$, 35.5° , 43.3° , 53.4° , 57.2°, and 62.5° correspond to the (220), (311), (400), (422), (511), and (440) planes, respectively. These peaks are characteristic reflections of magnetite with a cubic spinel structure (JCPDS card no. 19-0629). The presence of these well-defined peaks confirms the successful synthesis of crystalline Fe₃O₄ nanoparticles with high phase purity. Notably, no additional peaks were detected, indicating the absence of other iron oxide phases, such as hematite (α-Fe₂O₃) or maghemite (γ-Fe₂O₃) [21,22]. The sharp and intense diffraction signals further illustrate the good crystallinity of the nanoparticles, which contributes to structural stability during adsorption applications. These findings align with previous studies on Fe₃O₄ nanomaterials used as magnetic adsorbents, which reported similar diffraction patterns [21,22,23]. The confirmation of magnetite crystallinity through XRD is crucial, as it directly influences the magnetic properties of Fe_3O_4 , enabling efficient separation of the adsorbent after wastewater treatment [21,23].

VSM analysis

The magnetic properties of the synthesized Fe₃O₄ nanoparticles were investigated through Vibrating Sample Magnetometry (VSM), with the results illustrated in Figure 5. The nanoparticles exhibited a saturation magnetization (Ms) of 86.83 emu/g, aligning with the established range for Fe₃O₄-based nanoparticles [26]. High magnetic strength indicates the potential for efficient separation of the nanoparticles from aqueous solutions after the adsorption process by utilizing an external magnetic field [24,25]. Additionally, the absence of remanence and coercivity further confirms the superparamagnetic nature of these nanoparticles, which prevents agglomeration upon the removal of the magnetic field. [9]. This characteristic is particularly advantageous for wastewater treatment applications, as it ensures good dispersibility during adsorption while enabling simple, non-destructive recovery and potential reusability of the adsorbent.

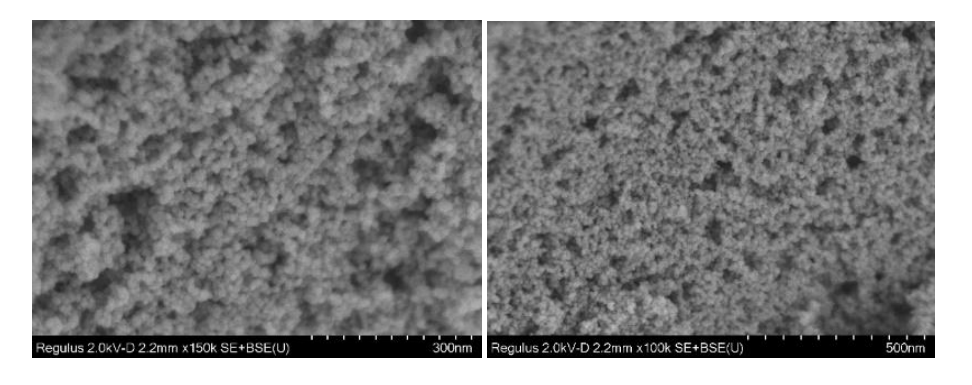


Figure 2. UHR-SEM images of Fe₃O₄ particles under 150k and 100k magnification

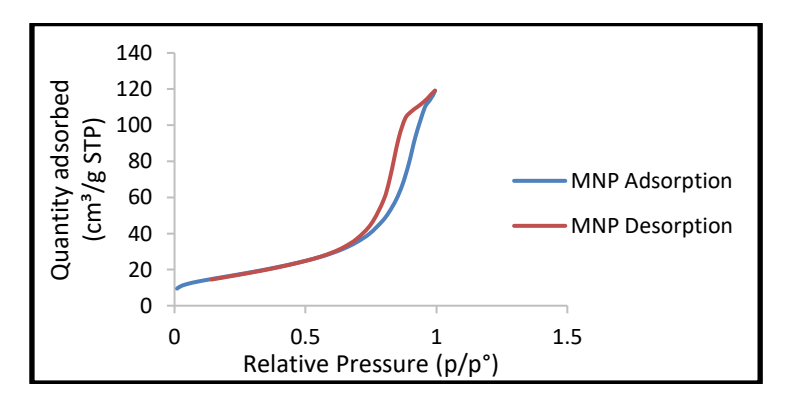


Figure 3. BET analysis of Fe₃O₄ particles

Malays. J. Anal. Sci. Volume 29 Number 5 (2025): 1554

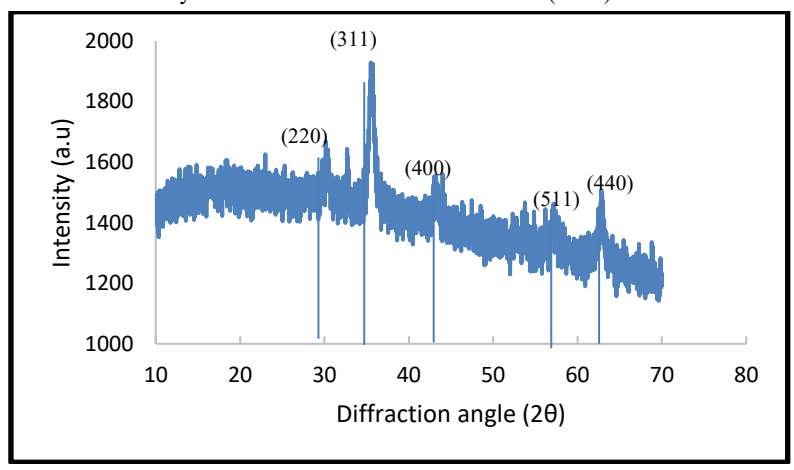


Figure 4. XRD pattern analysis on Fe₃O₄ particles

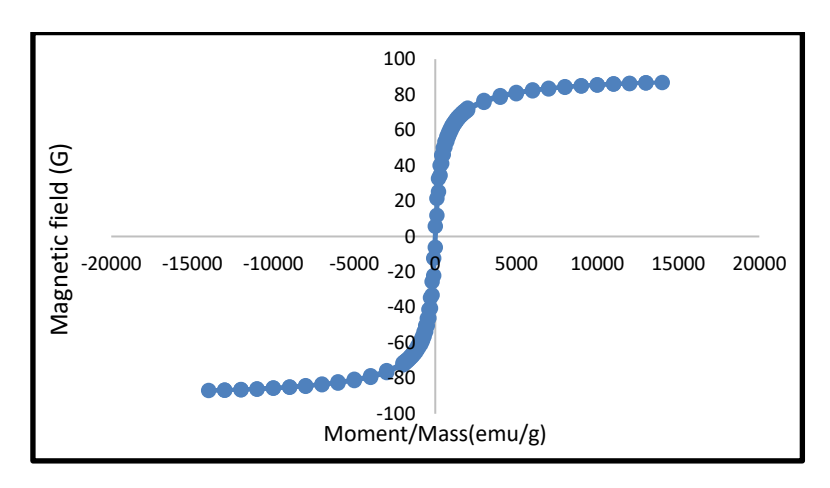


Figure 5. VSM analysis of Fe₃O₄ nanoparticles

Batch adsorption study

Various parameters, such as pH, mass adsorbent, and sample volume, were optimized by the Taguchi method. **Table 3** and **Figure 6** represent the results for the batch adsorption study of Allura red and Erioglaucine A using Fe₃O₄ nanoparticles.

The effect of the pH solution

The pH of a solution significantly influences the surface charge of Fe₃O₄ nanoparticles and the ionization states of dyes, both of which are critical in determining adsorption efficiency [17, 26]. This study focused on a pH range of 2–5, as detailed in Table 3 and illustrated in **Figure 6**, due to the notable adsorption observed in acidic conditions. The optimal removal percentage for Allura Red was achieved at pH 3, reaching 99.49% (S/N = 39.96), while Erioglaucine A showed maximum removal at pH 5, attaining 99.98% (S/N = 40.00).

For Allura Red, the solution's pH of 3 is significantly

below its pKa of 11.28, indicating that the dye predominantly exists in a protonated, non-ionized form at this acidic level [29]. This condition reduces the solubility of Allura Red due to the absence of strong polar interactions with water, thereby facilitating its partitioning onto Fe₃O₄ nanoparticles. Although some partial ionization may occur, certain functional groups (-SO₃-, -OH) can result in electrostatic attractions between the negatively charged residues of the dye and the positively charged nanoparticle surface under acidic conditions [9,28, 29]

At pH 5, Erioglaucine A exhibits partial ionization (pKa ≈ 5.63 –6.58). The presence of ionized sulfonate ($-SO_3$ –) and amine ($-NH_2$) groups enhances electrostatic interactions with Fe₃O₄, explaining the nearly complete removal of the dye [32]. The presence of negatively charged sulfonate groups under these conditions encourages favorable electrostatic interactions with the adsorbent surface, contributing to

the higher removal efficiency observed. These findings are consistent with existing literature, which indicates that the adsorption of dyes onto magnetic nanoparticles is highly dependent on pH, with acidic to near-neutral conditions being most conducive to optimal dye uptake [33].

The effect of Fe₃O₄ nanoparticles as an adsorbent

The mass of the adsorbent significantly affects the number of active sites available for dye adsorption. Data presented in **Table 3** and **Figure 6** demonstrate that the removal efficiency of Allura Red increased as the mass of Fe₃O₄ rose from 5 mg to 15 mg, but then decreased at 20 mg. A similar pattern was observed for Erioglaucine A, with adsorption peaking at 10 mg before declining at higher dosages.

The initial increase in efficiency can be attributed to the rising number of adsorption sites and functional groups available for binding [34]. Conversely, the decrease observed at higher mass levels may be linked to site saturation and mass transfer limitations. An excess of nanoparticles can lead to aggregation and uneven distribution of analyte molecules, which reduces the effective surface area and hinders adsorption, despite the increased adsorbent dosage [17,33].

The effect of solution volume

The volume of the solution also influences adsorption efficiency. **Table 3** shows that the removal efficiency for both dyes increased from 5 mL to 10 mL, achieving maximum effectiveness at 10 mL (99.86% for Allura Red and 100.22% for Erioglaucine A), followed by a decline beyond this volume.

This indicates that Fe₃O₄ has a limited adsorption capacity per unit volume [36]. In lower volumes (5 mL), the concentration of dye relative to the amount of adsorbent is insufficient, leading to an underutilization of active sites. At 10 mL, the balance between dye concentration and the available Fe₃O₄ surface groups maximize interactions between dye and adsorbent. However, larger volumes (≥15 mL) introduce an excess of dye molecules, which can saturate binding sites and leave some of the dye unabsorbed. Furthermore, higher volumes dilute the dye concentration per unit volume and increase the diffusion path length, thus reducing the likelihood of dye molecules contacting active sites. This collective impact results in diminished removal efficiency at higher sample volumes, aligning with earlier observations on the efficacy of nanoparticle-assisted dye removal [17, 27]. Therefore, 10 mL was identified as the optimal volume for the maximum removal of both dyes.

Based on the Table 3, each experimental run in the Taguchi design was conducted in triplicate, with average values. The removal efficiencies for Allura Red and Erioglaucine A dyes ranged from 63.52% to 100.66% and from 98.25% to 100.22%, respectively. The minimal difference between the highest and lowest values indicates a high degree of consistency across replicates, supporting that the variations observed are statistically significant rather than random. The maximum removal efficiency for Allura Red was achieved at pH 3, with 15 mg of Fe₃O₄ and a volume of 20 mL (100.66%). In contrast, the optimal conditions for Erioglaucine A were determined at pH 5, with 10 mg of Fe₃O₄ and a volume of 15 mL (100.22%). This consistency highlights the stability of the adsorption process across different parameter settings and demonstrates the strength of the Taguchi optimization method. Additionally, the S/N ratios clarify the magnitude of removal efficiency and its variability, explaining why higher percentage removals may sometimes coincide with lower S/N values, and vice versa [9,35].

The S/N ratio plotting

The Taguchi method utilizes the signal-to-noise (S/N) ratio as a logarithmic metric to improve process design by minimizing variability. Maximizing the signal-to-noise ratio is crucial for reducing the influence of uncontrollable factors on process performance [9, 36]. Table 4 provides a summary of the average S/N ratio values for each level of the factors studied, along with their ranks based on delta statistics, which reflect the relative impact of each factor [9, 36]. The table reveals that the mass of the adsorbent has a significant effect on the S/N ratio for Allura Red, while pH plays a dominant role for Erioglaucine A.

These findings are consistent with the trends shown in **Figure 6**, where the S/N ratios across various levels of each controllable factor are based on average removal efficiency. The most pronounced variation in the signal-to-noise ratio for Allura Red is associated with adsorbent mass, followed by pH and sample volume, which are important. Conversely, for Erioglaucine A, pH emerges as the primary factor, followed by adsorbent mass and sample volume. Overall, the results indicate that adsorbent mass and pH are the key factors affecting the removal of Allura Red and Erioglaucine A, respectively. At the same time, sample volume exerts minimal influence on both dyes.

Table 2. The percentage removal of Allura red and Erioglaucine A dyes in different treatments

No.	pН	MNPs (Fe ₃ O ₄)	Vol.	Average Removal (%)	Average Removal (%)
				Allura Red Dye	Erioglaucine A Dye
1	2	5	5	98.53	98.60
2	2	10	10	99.28	99.51
3	2	15	15	99.33	98.25
4	2	20	20	98.77	98.58
5	3	5	10	99.86	99.64
6	3	10	5	99.07	99.59
7	3	15	20	100.66*	98.44
8	3	20	15	98.38	99.26
9	4	5	15	92.95	99.94
10	4	10	20	98.98	99.90
11	4	15	5	98.65	99.84
12	4	20	10	97.90	99.24
13	5	5	20	63.52	100.11
14	5	10	15	98.53	100.22*
15	5	15	10	98.98	100.12
16	5	20	5	96.15	99.45

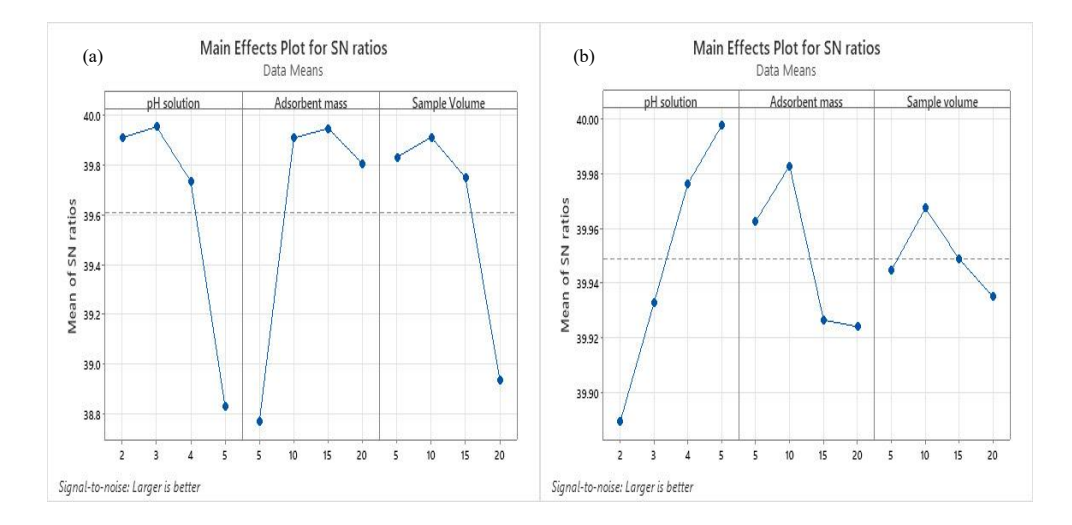


Figure 6. Response distribution of S/N ratio of Allura red (a) and Erioglaucine A (b) dye removals

Table 3. The table of the S/N ratio of main effects in Allura red and Erioglaucine A dye adsorption

		Allura Re	d	Erioglaucine A			
Level	pН	Adsorbent Mass	Sample Volume	pН	Adsorbent Mass	Sample Volume	
1	39.91	38.77	39.83	39.89	39.96	39.94	
2	39.95*	39.91	39.91*	39.93	39.98*	39.97*	
3	39.73	39.95*	39.75	39.98	39.93	39.95	
4	38.83	39.8	38.93	40.00*	39.92	39.93	
Delta	1.12	1.18	0.98	0.11	0.06	0.03	
Rank	2	1	3	1	2	3	

Application of ANOVA

The ANOVA analysis was conducted to evaluate the contribution of each factor to the removal efficiency of Allura Red and Erioglaucine A dyes. This analysis assesses the reliability of the findings and ensures that the experiments were performed under controlled conditions [11]. According to Korake et al. [11] and Dandil [38], an error contribution of less than 50% indicates adequate control of the experimental system. This study revealed error contributions of 36.05% for Allura Red and 0.10% for Erioglaucine A, both of which fall within acceptable limits and thus confirm the reliability of the results.

Table 5 displays the F-values and p-values used to evaluate the statistical significance of each factor. The F-value represents the ratio of the mean square of a factor to the residual error, with higher values indicating a more substantial effect on the response. A factor is considered statistically significant if its p-value is below 0.05 [38]. For Allura Red, the highest contribution came from adsorbent mass at 25.01%, followed closely by pH at 21.88%. Although the p-values for these factors exceeded 0.05, suggesting insufficient statistical significance, their contribution percentages indicate that they still have a practical impact on removal efficiency. In contrast, for

Erioglaucine A, pH emerged as the primary factor, contributing 59.12% and exhibiting a statistically significant p-value of 0.011, thereby underscoring its critical role in influencing removal efficiency.

Effect on the contact period

The efficiency of dye removal through adsorption on Fe₃O₄ nanoparticles in aqueous solutions is influenced by several factors, including the availability of active sites, dye concentration, surface porosity, the presence of functional groups on Fe₃O₄, surface area, and electrostatic forces [39]. The removal percentages increase over time until equilibrium is achieved. Specifically, within 10 minutes, the removal efficiency for both dyes improves significantly when the initial concentration is set at 10 mg/L, with the pH adjusted to 3 and 5 for each respective dye (see Figure 7). The observed removal percentages demonstrate a progressive improvement until no significant changes occur. This indicates that while numerous active sites are initially available for adsorption, a limited number of vacant sites remain as dye molecules progressively occupy these through competitive adsorption [17,37]. The results were used to evaluate the adsorption kinetics of Fe₃O₄ nanoparticles concerning Allura Red and Erioglaucine A.

Table 4. Analysis of variance for Allura red and Erioglaucine A dye removal

Types of Dye	Variance Source	DF	SS	MS	F-ratio	P-value	% Contribution
	pН	3	3.33	1.11	1.12	0.379	21.88
	Adsorbent mass	3	3.81	1.27	1.33	0.309	25.01
Allura red	Sample volume	3	2.46	0.82	0.77	0.531	16.19
	Error	12	36.05	3			36.92
	Total	21	45.65				100
	pН	3	0.028	0.0093	5.78	0.011	59.12
	Adsorbent mass	3	0.0099	0.0033	1.06	0.401	20.99
Erioglaucine A	Sample volume	3	0.0022	0.00074	0.2	0.896	4.72
	Error	12	0.1	0.0083			15.17
	Total	21	0.14				100

DF: Degree of freedom, SS: Sum of squares, MS: Mean of square

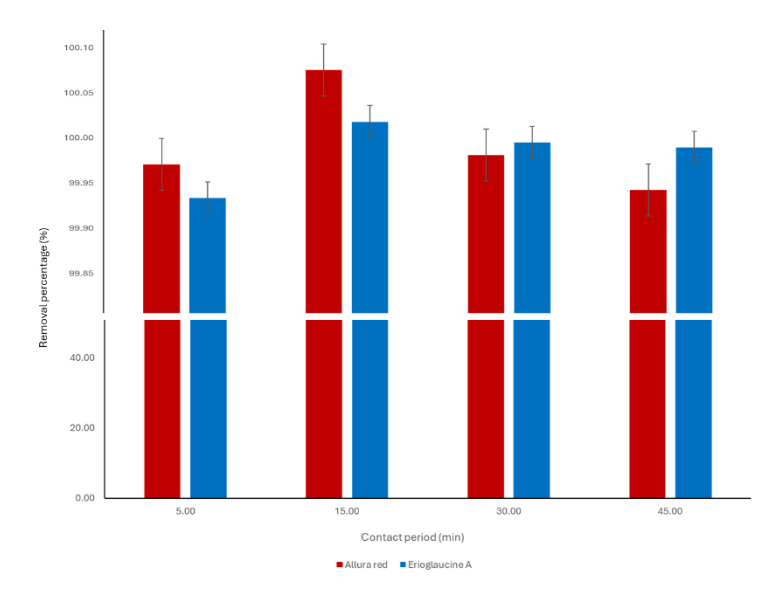


Figure 7. Effect of contact period on Allura red and Erioglaucine A dyes removal using Fe₃O₄. Condition: adsorbent amount: Allura red:15mg; Erioglaucine A:10 mg; Initial concentration:10 mg/L; sample solution volume: Allura red:10 mL; Erioglaucine A:10 mL; pH: Allura red: pH 3; Erioglaucine A:pH 5

Effect on initial concentration and temperature

Table 6 demonstrates the adsorption capacity and removal efficiency of Allura Red and Erioglaucine A dyes when utilizing Fe₃O₄ nanoparticles under varying initial concentrations (10 to 40 mg/L for Allura Red and 5 to 30 mg/mL for Erioglaucine A) and temperatures (298 K, 313 K, and 333 K). While removal percentages often approach 100%, important nuances arise, particularly concerning temperature and dye type.

Initially, the removal percentages for both dyes were comparable and notably high across different conditions, indicating that Fe₃O₄ nanoparticles exhibit a strong affinity for the dyes and effectively remove them from the solution, especially at lower concentrations. Percentages near 100% (99.55%, 99.94%, 99.87%) suggested that Fe₃O₄ nanoparticles have sufficient active sites to bind nearly all available dye molecules under the tested conditions [13,38].

However, the removal percentages can vary slightly due to the combined effects of initial concentration and temperature. For instance, at the highest temperature (333 K) and an initial concentration of 29.16 mg/mL, the removal percentage of Erioglaucine A drops to 69.15%. This significant decrease indicates that the nanoparticles' effectiveness for Erioglaucine A diminishes when exposed to higher temperatures and initial dye concentrations. In contrast, Allura Red maintains significantly high removal rates even at

333 K.

A noticeable decline in the removal percentage of Erioglaucine A is also recorded at 313 K with an initial concentration of 29.36 mg/L, where the removal percentage stands at 95.12%. This deviation from optimal removal suggests a possible onset of saturation or reduced efficiency, despite the high percentages [41].

The influence of temperature on adsorption capacity was evident and substantial for both dyes. Elevated temperatures enhance dye mobility, which increases the likelihood of dye molecules interacting with the active sites of Fe₃O₄ nanoparticles. This rise in adsorption capacity with temperature suggests that the adsorption process is endothermic. Increasing the temperature from 298 K to 313 K and then to 333 K has minimal impact on the maximum adsorption capacity of Allura Red at similar concentrations. At initial concentrations approximately 40-42 mg/L, the measured adsorption capacities were 28.16 mg/g at 298 K and 26.73 mg/g at 313 K.

At lower concentrations, the capacity remains relatively stable, measuring 6.72 mg/g at 298 K compared to 7.09 mg/g at both 313 K and 333 K for similar initial concentrations. The consistently high removal percentages suggest that higher temperatures do not significantly impede the adsorption of Allura

Red. This behavior indicates an endothermic adsorption process, whereby elevated temperatures provide additional energy for dye molecules to overcome activation barriers or enhance interactions with the adsorbent surface [40].

Conversely, for Erioglaucine A, higher temperatures typically have a detrimental effect, particularly at greater initial concentrations. While the adsorption capacity may remain stable or increase slightly at lower initial concentrations, the most significant finding is the sharp decline in removal percentage at 333 K. Although the adsorption capacity values for Erioglaucine A at elevated temperatures do not consistently fall below those at 298 K across all initial concentrations, the marked reduction in removal efficiency from 100% to 69.15% at 333 K for an initial concentration of 29.16 mg/L indicates that the adsorption process becomes less favorable at higher temperatures under these specific conditions. This suggests that the adsorption of Erioglaucine A may be exothermic, or that at elevated temperatures, the dye molecules gain enough kinetic energy to leave the adsorbent surface, or the stability of the adsorbed layer is compromised [40]. The table shows a removal percentage of 69.15% at 333 K, in contrast to significantly higher removal rates at 298 K and 313 K, despite similar initial concentrations.

The table further indicated that the maximum adsorption capacities were 28.16 mg/g for Allura Red and 28.64 mg/g for Erioglaucine A, measured at 298 K, occurring at their highest initial concentrations. A higher initial concentration leads to a larger concentration gradient, serving as a more effective driving force for transferring dye molecules from the bulk solution to the adsorbent surface. Greater availability of dye molecules allows for increased occupation of active sites, resulting in a higher total quantity of dye adsorbed per unit mass of the adsorbent until saturation occurs [19]. The significant adsorption capacity of Allura Red at elevated temperatures suggests that the process is either more endothermic or less susceptible to thermal desorption.

The lowest observed adsorption capacities were 6.72 mg/g for Allura Red and 5.80 mg/g for Erioglaucine A, consistently noted at the lowest initial concentrations. The amount of dye adsorbed is low due to the minimal initial concentration of dye in the system. As a result, the adsorbent remains significantly unsaturated under these conditions.

Thermodynamics study

In order to better understand the effect of temperature on dye removal, thermodynamic studies were employed by estimating the changes in standard Gibbs free energy (ΔG°), enthalpy (ΔH°), and entropy (ΔS°)

of adsorption. **Table 7** presents the thermodynamic parameters related to the adsorption of Allura Red and Erioglaucine A on Fe₃O₄ nanoparticles. According to Bıyıkoğlu [18], a negative enthalpy change ($\Delta H^{\circ} < 0$) indicates an exothermic process, whereas a positive change ($\Delta H^{\circ} > 0$) denotes an endothermic process. Additionally, a positive entropy change ($\Delta S^{\circ} > 0$) signifies an increase in randomness at the solid–solute interface, while a negative ΔS° suggests a reduction in randomness. The Gibbs free energy change (ΔG°) reflects the spontaneity of the adsorption process; negative ΔG° values confirm spontaneous adsorption. Values of ΔG° ranging from 0 to –20 kJ·mol⁻¹ suggest physical adsorption, while values between –80 and –400 kJ·mol⁻¹ are indicative of chemisorption.

This study demonstrates that the adsorption of Allura Red and Erioglaucine A consistently yields negative ΔG° values across all tested temperatures, confirming that the process is spontaneous. The negative ΔH° values further indicate that the adsorption of both dyes is exothermic. The entropy change (ΔS°) differs between the two systems: Allura Red exhibits a positive ΔS° , which points to increased molecular freedom and a more disordered arrangement at the interface, while Erioglaucine A displays a negative ΔS°, signifying decreased randomness and a more ordered structure during adsorption. This observed difference can likely be attributed to the larger molecular structure of Erioglaucine A, which may restrict its configurational mobility upon adsorption. The results indicate that both adsorption processes demonstrate thermodynamic stability, with adsorption of Allura Red primarily driven by entropy and that of Erioglaucine A governed by enthalpy, all while maintaining structural integrity at the solid-liquid interface [42].

Kinetics study

The study of adsorption kinetics is essential, as it provides valuable insights into the rate of adsorption, a critical factor in assessing adsorbent efficiency, while clarifying the fundamental mechanisms behind adsorption. This research examined the adsorption of Allura Red and Erioglaucine A onto Fe₃O₄ nanoparticles through five kinetic models: pseudofirst-order, pseudo-second-order, Elovich, intraparticle diffusion, and external diffusion.

Referring to **Table 8**, the pseudo-second-order model exhibited the strongest correlation with experimental data for both dyes. The calculated adsorption capacity for Allura Red (q_e , cal = 7.082 mg/g) closely matched the experimental value (q_e ,exp = 7.084 mg/g), reflecting a high correlation coefficient ($R^2 = 1.000$) and minimal relative error. Similarly, Erioglaucine A displayed a comparable kinetic trend, with q_e , cal

(11.111 mg/g) aligning closely with q_e ,exp (11.113 mg/g), yielding $R^2 = 1.000$ and negligible error. These results indicated that the adsorption of both dyes follows a pseudo-second-order mechanism, predominantly characterized by chemical interaction between the dye molecules and the Fe₃O₄ surface [18].

In contrast, the pseudo-first-order model proved insufficient, demonstrated by a weak correlation (R² <0.33) and significant discrepancies between

experimental and calculated adsorption capacities, with relative errors exceeding 90%. The Elovich and intra-particle diffusion models showed moderate correlations, indicating that while surface interactions and diffusion may contribute to the process, they are not the primary mechanisms at play. Additionally, external diffusion exhibited a weak correlation (R² <0.28), further affirming its minimal role in the rate-controlling step [43].

Table 5. Effect of initial solution concentration and temperature on (a) Allura red removal and adsorption capacity. Condition: adsorbent amount: 15 mg; contact period:15 min; volume of sample:10 mL; pH 3, (b) Erioglaucine A removal and adsorption capacity. Condition: adsorbent amount: 10 mg; contact period:10 min; volume of sample:10 mL; pH 5.

Type of Dye (s)	Temperature	Initial concentration (mg/L)	Removal Percentage (%)	Adsorption Capacity (mg/g)
		10.08	100.00	6.72
	298K	21.26	99.55	14.11
	290K	31.10	100.00	20.73
		42.24	100.00	28.16
		10.63	100.00	7.09
Allura red	313K	20.60	100.00	13.73
Allura red	313K	31.02	100.00	20.68
		40.10	100.00	26.73
		10.63	99.94	7.09
	333K	20.60	100.00	13.73
		31.02	100.00	20.68
		40.10	100.00	26.73
		5.80	100.00	5.80
	298K	10.86	99.87	10.85
		21.36	100.00	21.36
		29.36	97.55	28.64
		5.80	100.00	5.80
Erioglaucine A	313K	10.86	100.00	10.86
Eriogiaucine A	313IX	21.36	100.00	21.36
		29.36	95.12	27.92
		5.66	100.00	5.66
	333K	11.36	100.00	11.36
	333 IX	19.57	99.97	19.56
		29.16	69.15	20.17

Malays. J. Anal. Sci. Volume 29 Number 5 (2025): 1554 **Table 6.** Thermodynamics parameters for Allura red and Erioglaucine A adsorption process

		Van H	off Plot	Plot The value of Enthalpy, Entr			py, Entropy, and Fr	, Entropy, and Free Gibbs Energy	
Types of Dye	T(K)	1/T X 10^3	Final	Capacity (q)	kd	ln k _d	Enthalpy, ∆H° J/mol	Entropy, ∆S° J/Kmol	Gibbs energy, ∆G kJ/mol
	298	3.36	0.0010	28.16	28162.70	10.25			-25384.59
Allura red	313	3.14	0.0010	26.73	26730.70	10.19	-1.11	81.38	-26526.54
	333	2.96	0.0010	26.73	26730.70	10.19			-28221.52
	298	3.36	0.72	28.64	39.79	3.68			-9126.64
Erioglaucine A	313	3.14	1.43	27.92	19.50	2.97	-59.52	-166.98	-7729.76
	333	2.96	9.00	20.17	2.24	0.81			-2234.33

The kinetic analysis indicated that the adsorption of Allura Red and Erioglaucine A onto Fe₃O₄ nanoparticles adheres to pseudo-second-order kinetics. This finding underscored chemical interaction as the principal mechanism, with the adsorption rate primarily influenced by the availability of active binding sites and strong molecular interactions between the dyes and the nanoparticle surfaces, rather than by limitations in mass transfer.

Isotherm study

Isotherm studies are critical for understanding the adsorption process, as they provide valuable insights into the interactions between adsorbates and the surfaces of adsorbents, as well as the capacity, energy, and mechanisms involved in adsorption. This investigation focused on evaluating the adsorption behaviors of Allura Red and Erioglaucine A on Fe₃O₄ nanoparticles, employing five classical isotherm models: Langmuir, Freundlich, Temkin, Dubinin-Radushkevich (D-R), and Halsey at a temperature of 298 K, as presented in Table 9. Selecting an appropriate isotherm model is vital, as it elucidates the underlying adsorption mechanism, which may involve monolayer or multilayer formation, homogeneous or heterogeneous surface binding, as well as the predominance of physical or chemical adsorption.

The results indicated that the Langmuir model was the most accurate representation of the adsorption process for Allura Red, achieving a perfect correlation coefficient ($R^2 = 1.000$) at 298K with a maximum

adsorption capacity of 14.1044 mg/g. This strong correlation suggests that the adsorption of Allura Red occurs via monolayer coverage on a homogeneous surface characterized by identical and energetically equivalent binding sites [18]. Furthermore, the Langmuir separation factor (R^L) recorded values of 1, implying a linear adsorption behavior [38]. This suggests that while the adsorption is effective, it is not classified as a highly spontaneous process under the experimental conditions. Other models, including Freundlich, Temkin, D–R, and Halsey, displayed inadequate fits, with R² values ranging from 0.0081 to 0.0584, indicating that the adsorption process does not conform to multilayer or heterogeneous surface mechanisms [14].

Similarly, the Langmuir isotherm was determined to effectively describe the adsorption of Erioglaucine A, with a correlation coefficient (R2) of 0.999 at 298 K, with a maximum adsorption capacity of 28.9017 mg/ g, further supporting the notion of monolayer adsorption on a homogeneous surface [18]. The q_m value for Erioglaucine A is higher than that for Allura Red, suggesting a stronger interaction and a higher affinity of Fe₃O₄ nanoparticles towards Erioglaucine A molecules. However, the Freundlich model fell short in characterizing Erioglaucine A adsorption due to negative parameter values and low R2 scores. Likewise, the Temkin, D-R, and Halsey models were ineffective, exhibiting significantly weaker correlations.

The comparative analysis of the isotherm models indicates that the Langmuir isotherm is the most

suitable descriptor of dye adsorption on Fe₃O₄ nanoparticles for both Allura Red and Erioglaucine A. The high correlation coefficients ($R^2 \geq 0.999$) substantiate the assumptions of the Langmuir model involving monolayer adsorption and uniform active

sites. These findings underline the predictive capability of the Langmuir model in characterizing the equilibrium behavior of dye adsorption systems, contributing significant insights for the design and optimization of nanoparticle-based adsorbents in wastewater treatment applications.

Table 7. The parameters in the adsorption process for Allura red and Erioglaucine A based on kinetic studies

		Allura Red	Erioglaucine A
Kinetic models	Parameters	Materials	Materials
		MNP	MNP
	q _e exp (mg/g)	7.08467	11.113
Pseudo-first order	q _e cal (mg/g)	9.4624×10 ⁻⁷	0.1377
	K ₁ min ⁻¹	-0.1617	-0.175
	\mathbb{R}^2	0.1291	0.3296
	q (%)	57.745	57.0196
	Relative error (%)	100	98.7609
Pseudo-second order	q _e cal (mg/g)	7.08215	11.111
	K ₂ (g/mg min)	-22.153	81.0016
	h (mg/g min)	-1111.1	10000
	t^1/2 (min)	-3.128	7.2902
	\mathbb{R}^2	1	1
	q (%)	0.02051	0.01039
	Relative error (%)	0.03552	0.018
Elovich equation	qe cal (mg/g)	7.0828	11.11
	B (g/mg)	-1428.6	370.37
	a (mg/g min)	0	0
	\mathbb{R}^2	0.1392	0.5176
	q (%)	0.01518	0.01559
	Relative error (%)	0.02629	0.027
Intra-particle diffusion	C (mg/g)	7.0848	11.106
	K (mg/gmin)	-0.0004	0.0013
	\mathbb{R}^2	0.2608	0.4035
External diffusion	K ext (1/min)	-0.0648	-0.2159
	C (mg/g)	-4.505	-3.1256
	\mathbb{R}^2	0.0783	0.2777

Table 8. Parameters of the Freundlich, Langmuir, Halsey, Temkin, and Dubinin-Radushkevich isotherms for the Allura red and Erioglaucine A adsorption at 298 K

Isotherm Models	Parameters	Allura Red	Erioglaucine A
Langmuir	$q_m \left(mg/g \right)$	14.1044	28.9017
	b (L/mg)	0	115.333
	\mathbb{R}^2	1	0.999
	$R_{ m L}$	1	2.17E-4
Freundlich	K_F ((mg/g) (L/mg)1/n)	15.7725	15.0973
	n	20.9644	15.1976
	1/n	0.0477	0.0658
	\mathbb{R}^2	0.0081	0.0365
Temkin	$K_{T}\left(L/mg\right)$	17731.7	100722
	$b_T(kJ/mol)$	1307.43	1542.89
	\mathbb{R}^2	0.0584	0.1051
Dubinin-Radushkevich	$q_m \left(mg/g \right)$	15.773	15.1773
	b (L/mg)	0.0031	0.0028
	\mathbb{R}^2	0.0081	0.0454
	E	35.9211	0.1058
Halsey	N	-20.964	-15.198
	K	7.70E-26	-41.255
	\mathbb{R}^2	0.0081	0.0365

Method validation

The method validation was evaluated based on several parameters, including linear dynamic range (LDR), precision, accuracy, percentage recovery (%R), and selectivity. Linearity was assessed by constructing calibration curves for the concentrations of Allura Red and Erioglaucine A dyes. The method demonstrated linearity over concentration ranges of 5 mg/mL to 30 mg/L for Erioglaucine A and 2 mg/mL to 40 mg/L for Allura Red (see **Table 10**).

Precision was determined by analyzing three replicates at three different concentrations on the same day and subsequently across three different days at the same concentrations. The relative standard deviation (%RSD) was calculated based on the results obtained.

The mean percentage recovery for each nominal concentration, derived from three replicates, indicates the accuracy of the measurements. In order to obtain accuracy, three food industrial wastewater samples were spiked with three different concentrations of Allura Red (10, 25, and 40 mg/L) and Erioglaucine A (5, 15, and 30 mg/L). The R² value obtained from the plot of absorbance value against the concentration of analyte for both dyes Erioglaucone A and Allura red were 0.997 and 0.999.

Analysis of real samples

The study investigated the adsorption capacity of Fe₃O₄ nanoparticles to remove Allura Red and Erioglaucine A in actual wastewater samples, focusing on potential matrix effects. Three wastewater samples sourced from the food industry in the Penang area were spiked with varying concentrations of Allura Red (10, 25, and 40 mg/L) and Erioglaucine A (5, 15, and 30 mg/L). Results, as summarized in Table 11, indicated that the removal efficiency for Allura Red consistently ranged from 94.57% to 100.13%, with relative standard deviations (RSD) between 0.00% and 1.34%. This demonstrates both the efficiency and reproducibility of the adsorption process. In contrast, the removal of Erioglaucine A revealed greater variability, with efficiencies fluctuating from 1.19% to 100.08% and RSD values below 35%, indicating a higher sensitivity to concentration and matrix effects

The superior and more consistent removal rates for Allura Red, as opposed to Erioglaucine A, can be attributed to differences in their molecular structures [29]. Allura Red possesses a smaller and less bulky configuration, promoting enhanced accessibility to active sites on the Fe₃O₄ nanoparticles and facilitating stronger electrostatic interactions. Its sulfonate groups (-SO₃⁻) can form strong electrostatic interactions with

the surface Fe^{2+}/Fe^{3+} sites of the nanoparticles, while additional hydrogen bonding and possible $\pi-\pi$ stacking interactions between the aromatic rings of Allura Red and the Fe_3O_4 surface enhance binding affinity. In contrast, Erioglaucine A, being bulkier and more structurally complex with multiple aromatic substituents, experiences steric hindrance that reduces its ability to approach and anchor effectively onto the Fe_3O_4 surface. Although Erioglaucine A also contains sulfonate groups capable of electrostatic binding, its larger molecular size and extended structure hinder optimal surface interaction, leading to lower overall adsorption efficiency [42,43]. This structural limitation results in lower adsorption efficiency when compared to Allura Red.

Additionally, the concentration of the dye significantly influenced the adsorption behavior of Erioglaucine A. At lower concentrations, the available adsorption sites on the Fe₃O₄ nanoparticles were sufficient to accommodate the dye molecules, leading to high removal efficiencies [13,38]. However, at high concentrations 30 mg/L), competitive (e.g., interactions among Erioglaucine A molecules for the limited active sites became more pronounced, while hindrance further limited adsorption, culminating in a notable decline in efficiency. This observation is consistent with Langmuir adsorption theory, which posits that adsorption capacity is finite, and at higher solute concentrations, multilayer adsorption or incomplete surface coverage may occur [12, 16].

Table 9. Linearity and repeatability results of Allura red and Erioglaucine A removal method

Types of Dye	\mathbb{R}^2	Spiked Levels (mg/mL)	Intra-day (n=5) Average Removal (%)	Average RSD (%)	Inter-day (n=3) Average Removal (%)	Average RSD (%)
		10	100.28	0.14	100.1	0.16
Allura red	0.999	25	100.09	0.05	100.04	0.04
		40	99.97	0.11	99.89	0.17
		5	100.02	0.09	100.02	0.1
Erioglaucine A	0.997	15	100.02	0.02	100.03	0.03
2.1		30	65.41	10.04	66.68	10.19

Table 10. Removal percentage efficiency of Allura red and Erioglaucine A in real samples on Fe₃O₄ adsorbent

Wastewater	Spiked Levels	Allura red	Spiked Levels	Erioglaucine A
	(mg/mL)	Removal (%) ± RSD	(mg/mL)	Removal (%) ± RSD
Location A	10	100.13 ± 0.03	5	100.08 ± 0.02
	25	100.07 ± 0.00	15	99.49 ± 0.71
	40	100.05 ± 0.01	30	1.19 ± 11.38
Location B	10	100.09 ± 0.09	5	26.87 ± 12.70
	25	99.85 ± 0.24	15	18.76 ± 8.65
	40	94.57 ± 1.34	30	1.76 ± 30.27
Location C	10	100.11 ± 0.06	5	98.16 ± 2.69
	25	100.05 ± 0.01	15	81.09 ± 3.56
	40	100.00 ± 0.02	30	2.86 ± 19.18

Reusability

The reusability of Fe₃O₄ nanoparticles was evaluated through adsorption and desorption cycles to determine their potential as economical and sustainable adsorbents. After each adsorption cycle, the exhausted adsorbent was regenerated using methanol, magnetically separated, and then dried for reuse. The

performance of regeneration showed varying behaviors for Allura Red and Erioglaucine A.

Figure 12 demonstrates that the removal efficiency of Allura Red remained exceptionally high, with only a minimal decrease (99.88% after the 20th cycle). This

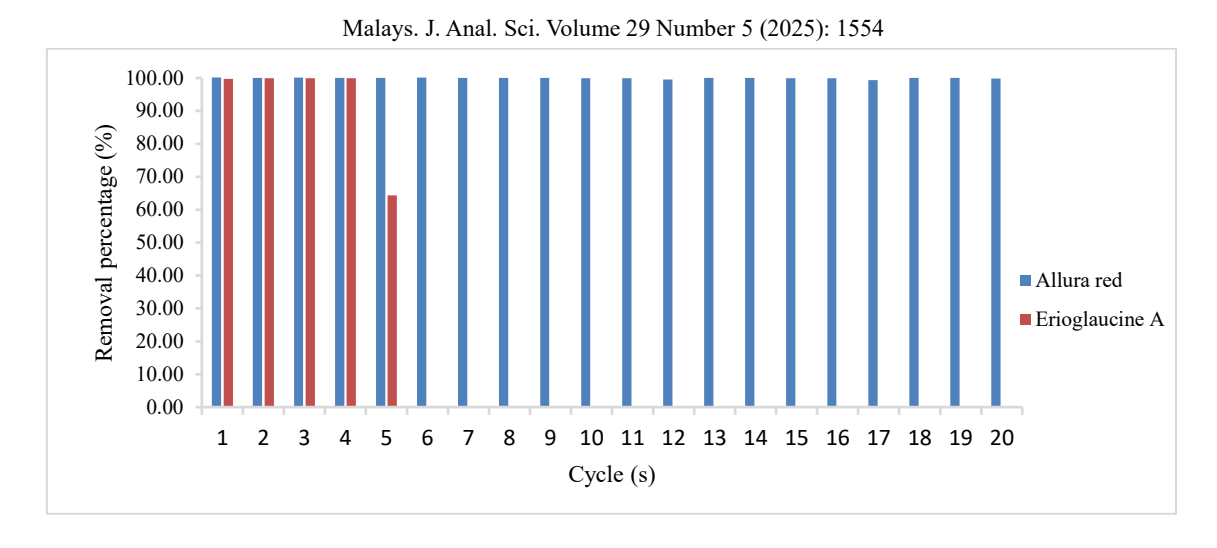


Figure 3 Reusability of Allura red and Erioglaucine A removal in different runs

consistent performance can be attributed to the favourable interactions between Allura Red and Fe₃O₄ nanoparticles. Under acidic conditions, the surface of Fe₃O₄ undergoes ionization (Fe⁺), which creates positively charged sites that electrostatically attract Allura Red's negatively charged sulfonate groups. In addition to electrostatic forces, hydrogen bonding and van der Waals interactions stabilize the dye-adsorbent complex. Acidic conditions do not alter the geometric surface area of Fe₃O₄; instead, they enhance the functional adsorption area by activating additional surface sites, which increases the adequate adsorption capacity [8,17,26]. The combination of strong yet reversible adsorption allows for effective desorption using methanol, enabling the reuse of Fe₃O₄ with negligible loss in efficiency. The slight decrease observed is likely due to minor adsorbent loss during handling rather than a reduction in adsorption affinity.

In contrast, the reusability of Fe₃O₄ for Erioglaucine A was limited to five cycles, with removal efficiency dropping significantly to 64.38%. This reduction is primarily due to the bulkier and sterically hindered structure of Erioglaucine A, which restricts access to adsorption sites and weakens the electrostatic interactions compared to Allura Red. After the fifth adsorption showed the decreased reproducibility, indicating that the available active sites were increasingly obstructed or rendered inaccessible [45]. The study was constrained to five cycles due to a significant decline in adsorption efficiency, making further testing insignificant regarding performance outcomes.

The findings indicated that the efficiency of adsorption and reusability of Fe₃O₄ nanoparticles are significantly affected by the structure of the dye and the nature of dye-adsorbent interactions. Allura Red

shows superior reusability across multiple cycles, attributed to its smaller size and favorable interaction with protonated Fe₃O₄ surfaces. In contrast, Erioglaucine A exhibits limited recyclability due to steric hindrance and weaker interaction forces. Overall, this research suggests that Fe₃O₄ nanoparticles, particularly in the context of Allura Red, serve as a stable, economical, and environmentally sustainable adsorbent for various wastewater treatment applications.

Conclusion

In summary, this research demonstrated the effectiveness of Fe₃O₄ nanoparticles as adsorbents for the extraction of Allura Red and Erioglaucine A dyes from aqueous solutions. The nanoparticles exhibited a uniform spherical morphology, mesoporosity, and strong magnetic properties, as confirmed by physicochemical characterization. Using the Taguchi method for process optimization, a maximum removal efficiency of 100.66% for Allura Red was achieved under the following conditions: pH 3, 15 mg of adsorbent, and a volume of 20 mL. In comparison, Erioglaucine A reached a removal efficiency of 100.22% at pH 5, utilizing 10 mg of adsorbent and a volume of 15 mL. Analysis of the signal-to-noise ratio revealed that the mass of the adsorbent and pH were the most significant factors for removing Allura Red and Erioglaucine A, respectively. At the same time, sample volume had a negligible effect. Notably, significant dye removal occurred within 10 minutes at low concentrations, and higher temperatures further improved adsorption capacity due to enhanced dye mobility.

Thermodynamic analysis indicated that the adsorption of both dyes was spontaneous, exothermic, and primarily driven by chemisorption. The maximum adsorption capacities were 7.082 mg/g for Allura Red

and 11.111 mg/g for Erioglaucine A. The pseudo-second-order model best represented the kinetics of adsorption. The Langmuir isotherm provided the best fit for both dyes, evidenced by high correlation coefficients ($R^2 = 0.999$ for Allura Red and 0.997 for Erioglaucine A) and a precision level below 15%.

Reusability studies showed that Allura Red maintained excellent stability with consistent removal efficiency across 20 cycles. In contrast, Erioglaucine A exhibited limited reusability, achieving only five cycles, likely due to its bulkier structure, which hinders interaction with the active sites of Fe₃O₄. Validation with actual wastewater samples indicated removal efficiencies ranging from 94.57% to 100.13% for Allura Red and 1.19% to 100.08% for Erioglaucine A. This confirms the efficacy of Fe₃O₄ nanoparticles as a viable adsorbent for treating dye-contaminated effluents.

Acknowledgement

The authors would like to express their gratitude to the Ministry of Higher Education, Malaysia, for providing funding for this project through the Fundamental Research Grant Scheme (FRGS) with reference code FRGS/1/2021/STG04/USM/02/8 and account code 203.CIPPT.6711974. The authors are also thankful to the Advanced Medical and Dental Institute, Universiti Sains Malaysia, for providing the necessary resources to complete this project.

References

- Tan, K. B., Vakili, M., Horri, B. A., Poh, P. E., Abdullah, A. Z. and Salamatinia, B. (2015). Adsorption of dyes by nanomaterials: Recent developments and adsorption mechanisms. Separation Purification. Technology, 150: 229-242.
- Jusoh, N., Othman, N., and Bukhari Rosly, M. (2020). Extraction and recovery of organic compounds from aqueous solution using emulsion liquid membrane process. *Material Today Proceedings*, 47: 1301-1306.
- 3. Panda, S.K., Aggarwal, I., Kumar, H., Prasad, L., Kumar, A., Sharma, A., Vo, D.N., Thuan, D.V., and Mishra, V. (2021). Magnetite nanoparticles as sorbents for dye removal: a review. *Springer International Publishing*, 19(3): 2487-2525.
- Załuski, D., Stolarski, J. M., and Krzyżaniak, M. (2022). Validation of the Taguchi method on the example of evaluation of willow biomass production factors under environmental stress. *Industrial Crops and Products*, 185: 115170.
- Husin, N. A., Hashim, N. M., Yahaya, N., Miskam, M., Raoov, M., and Zain, N. N. M. (2021). Exploring magnetic particle surface embedded with imidazole-based deep eutectic solvent for diclofenac removal from

- pharmaceutical wastewater samples. *Journal of Molecular Liquids*, 332: 115809.
- Dutta, S., Gupta, B., Srivastava, S. K., and Gupta, A. K. (2021). Recent advances on the removal of dyes from wastewater using various adsorbents: A critical review. *Materials Advances*, 2(14): 4497-4531.
- Mohammad Razi, M. A., Mohd Hishammudin, M. N. A., and Hamdan, R. (2017). Factor affecting textile dye removal using adsorbent from activated carbon: a review. MATEC Web Conference, 103: 1-17.
- Rashid, H., Mansoor, M. A., Haider, B., Nasir, R., Abd Hamid, S. B., and Abdulrahman, A. (2020). Synthesis and characterization of magnetite nano particles with high selectivity using in-situ precipitation method. Separation Science and Technology, 55(6): 1207-1215.
- Queiros Campos, J., Checa-Fernandez, B.L., Marins, J. A., Lomenech, C., Hurel, Ch., Godeau, G., Raboisson-Michel, M., Verger-Dubois, G., Bee, A., and Talbot, D., and Kuzhir, P.J. (2021). Adsorption of organic dyes on magnetic iron oxide nanoparticles. part II: fieldinduced nanoparticle agglomeration and magnetic separation. *Langmuir*, 37(35): 10612-10623.
- Jokić, A., Petković, B., Jevtić, S., Vasić, V., and Laban, B. (2019). Characterization of new synthesized Fe2O3 nanoparticles and their application as detection signal amplifiers in herbicide bentazone electroanalytical determination. *University Thought - Publication* in Natural Sciences, 9(1): 27-31.
- 11. Korake, R., and Jadhao, P. D. (2021). Investigation of Taguchi optimization, equilibrium isotherms, and kinetic modeling for cadmium adsorption onto deposited silt. *Heliyon*, 7: e05755.
- 12. Pundir, R., Chary, G. H. V. C., and Dastidar, M. G. (2018). Application of Taguchi method for optimizing the process parameters for the removal of copper and nickel by growing Aspergillus sp.. *Water Resources and Industry*, 20: 83-92.
- Essa, W. K., Yasin, S. A., Abdullah, A. H., Thalji, M. R., Saeed, I. A., Assiri, M. A., Chong, K. F., and Ali, G. A. M. (2022). Taguchi L25 (5⁴) approach for methylene blue removal by polyethylene terephthalate nanofiber-multiwalled carbon nanotube composite. *Water*, 14 (8): 1242.
- 14. Sumanjit, Rani, S., and Mahajan, R. K. (2016). Equilibrium, kinetics and thermodynamic parameters for adsorptive removal of dye Basic Blue 9 by ground nut shells and Eichhornia. *Arabian Journal of Chemistry*, 9: S1464–S1477.
- 15. Ali, A., Zafar, H., Zia, M., ul Haq, I., Phull, A.

- R., Ali, J. S., and Hussain, A. (2016). Synthesis, characterization, applications, and challenges of iron oxide nanoparticles. *Nanotechnology, Science and Applications*, 9(4): 49-67.
- 16. Mosoarca, G., Popa, S., Vancea, C., and Boran, S. (2021). Optimization, equilibrium and kinetic modeling of methylene blue removal from aqueous solutions using dry bean pods husks powder. *Materials*, 14(19): 5673.
- Khan, A., Begum, S., Ali, N., Khan, S., Hussain, S., and Sotomayor., M. D. P. T. (2017). Preparation of crosslinked chitosan magnetic membrane for cations sorption from aqueous solution. *Water Scienc & Technology*, 75(9): 2034-2046.
- 18. Bıyıkoğlu, M. (2025). Innovative approaches in wastewater treatment: kinetic and isotherm investigation of dye adsorption on sulfurmodified PET fibers. *Research on Chemical Intermediates*, 51(6): 3281-3299.
- Giri, S. K., Das, N. N., and Pradhan, G. C. (2011). Synthesis and characterization of magnetite nanoparticles using waste iron ore tailings for adsorptive removal of dyes from aqueous solution. *Colloids and Surfaces A: Physicochemical and Engineering Aspects*, 389: 4908.
- 20. Abebe, B., Murthy, H. C. A., and Amare, E. (2018). Summary on adsorption and photocatalysis for pollutant remediation: mini review. *Journal of Encapsulation and Adsorption Sciences*, 8(4): 225-255.
- 21. Sotomayor, F., Quantatec, A. P., Sotomayor, F. J., Cychosz, K. A., and Thommes, M. (2018). Characterization of micro/mesoporous materials by physisorption: concepts and case studies. *Accounts of Materials and Surface Research*, 3(2): 34-50.
- Waheed, A., Mansha, M., Kazi, I. W., and Ullah, N. (2019). Synthesis of a novel 3,5diacrylamidobenzoic acid based hyper-crosslinked resin for the efficient adsorption of Congo Red and Rhodamine B. *Journal of Hazardous Materials*, 369(2): 528-538.
- Masuku, M., Ouma, L., and Pholosi, A. (2021). Microwave assisted synthesis of oleic acid modified magnetite nanoparticles for benzene adsorption. *Environmental Nanotechnology, Monitoring and Management*, 15(9): 100429.
- 24. Fan, L., Luo, C., Li, X., Lu, F., Qiu, H., and Sun, M. (2012). Fabrication of novel magnetic chitosan grafted with graphene oxide to enhance adsorption properties for methyl blue. *Journal of Hazardous Materials*, 215-216: 272-279.
- Mohamed, A., Atta, R. R., Kotp, A. A., Abo El-Ela, F. I., Abd El-Raheem, H., Farghali, A., Alkhalifah, D. H. M., Hozzein, W. N., and Mahmoud, R. (2023). Green synthesis and

- characterization of iron oxide nanoparticles for the removal of heavy metals (Cd²⁺ and Ni²⁺) from aqueous solutions with Antimicrobial Investigation. *Scientific Reports*, 13(1): 1-30.
- Damasceno, B. S., da Silva, A. F. V., and de Araújo, A. C. V. (2020). Dye adsorption onto magnetic and superparamagnetic Fe₃O₄ nanoparticles: A detailed comparative study. *Journal of Environmental Chemical Engineering*, 8: 103994.
- Hadadian, Y., Masoomi, H., Dinari, A., Ryu, C., Hwang, S., Kim, S., Cho, B. K., Lee, J. Y., and Yoon, J. (2022). From low to high saturation magnetization in magnetite nanoparticles: the crucial role of the molar ratios between the chemicals. ACS Omega, 7: 15996.
- 28. Saif, S., Tahir, A., and Chen, Y. (2016). Green synthesis of iron nanoparticles and their environmental applications and implications. *Nanomaterials*, 6(11): 1-26.
- 29. Şen, N. E., and Şenol, Z. M. (2023). Effective removal of Allura red food dye from water using cross-linked chitosan-diatomite composite beads. *International Journal of Biological Macromolecules*, 253(5): 126632.
- Başar, C. A., Korkmaz, A. A., Önal, Y., and Utku, T. (2022). Evaluation of optimum carbonization conditions of the blended domestic polymeric waste, biomass and lignite in the presence of catalyst by Taguchi and ANOVA optimization analysis. *Journal of Hazardous Materials Advances*, 8: 100164.
- 31. Liu, X., Tian, J., Li, Y., Sun, N., Mi, S., Xie, Y., and Chen, Z. (2019). Enhanced dyes adsorption from wastewater via Fe₃O₄ nanoparticles functionalized activated carbon. *Journal of Hazardous Materials*, 373(2): 397-407.
- Yu, D., Hu, Z. H., Wang, Y. G., Liang, X. X., Ouyang, X. K., and Omer, A. M. (2019). Efficient adsorption of diclofenac sodium from aqueous solutions using magnetic aminefunctionalized chitosan. *Chemosphere*, 217: 270-278.
- 33. Rouhani, M., Ashrafi, S. D., Taghavi, K., Joubani, M. N., and Jaafari, J. (2022). Evaluation of tetracycline removal by adsorption method using magnetic iron oxide nanoparticles (Fe₃O₄) and clinoptilolite from aqueous solutions. *Journal of Molecular Liquids*, 356: 119040.
- 34. Badruddoza, A. Z. M., Tay, A. S. H., Tan, P. Y., Hidajat, K., and Uddin, M. S. (2011). Carboxymethyl-β-cyclodextrin conjugated magnetic nanoparticles as nano-adsorbents for removal of copper ions: Synthesis and adsorption studies. *Journal of Hazardous Materials*, 185(2–3): 1177-1186
- 35. Behnajady, M. A., Bimeghdar, S., and Eskandarloo, H. (2018). Photocatalytic activity

- of Ag/TiO₂–P25 modified cement: Optimization using Taguchi approach. *Environmental Engineering and Management Journal*, 17(5): 1131-1138.
- 36. Dandil, S. (2024). Design of decolorization of methylene blue mixed synthetic wastewater via modified vermiculite using Taguchi method. *Adsorption Science and Technology*, 42.
- 37. Islam, M. A., Ahmed, M. J., Khanday, W. A., Asif, M., and Hameed, B. H. (2017). Mesoporous activated coconut shell-derived hydrochar prepared via hydrothermal carbonization-NaOH activation for methylene blue adsorption. *Journal of Environmental Management*, 203: 237-244.
- 38. Eleryan, A., Aigbe, U. O., Ukhurebor, K. E., Onyancha, R. B., Hassaan, M. A., Elkatory, M. R., Ragab, S., Osibote, O. A., Kusuma, H. S., and El Nemr, A. (2023). Adsorption of direct blue 106 dye using zinc oxide nanoparticles prepared via green synthesis technique. *Environmental Science and Pollution Research*, 30(26): 69666-69682.
- Nassar, N. N., Marei, N. N., Vitale, G., and Arar, L. A. (2015). Adsorptive removal of dyes from synthetic and real textile wastewater using magnetic iron oxide nanoparticles: Thermodynamic and mechanistic insights.

- Canadian Journal of Chemical Engineering, 93(11): 1965-1974
- 40. Yang, G., Gao, Q., Yang, S., Yin, S., Cai, X., Yu, X., Zhang, S., and Fang, Y. (2020). Strong adsorption of tetracycline hydrochloride on magnetic carbon-coated cobalt oxide nanoparticles. *Chemosphere*, 239.
- 41. Yang, J., and Han, S. (2018). Kinetics and equilibrium study for the adsorption of lysine on activated carbon derived from coconut shell. *Desalination and Water Treatment*, 120: 261-271.
- Osagie, C., Othmani, A., Ghosh, S., Malloum, A., Kashitarash Esfahani, Z., and Ahmadi, S. (2021). Dyes adsorption from aqueous media through the nanotechnology: A review. *Journal of Materials Research and Technology*, 14: 2195-2218.
- 43. Özgen, A., Dalmaz, A., and Sivrikaya Özak, S. (2025). A new method for the determination of Brilliant Blue FCF in energy drinks: Smartphone digital imaging colorimetry (SDIC) and green deep eutectic solvent-based dispersive microextraction procedure. *Microchemical Journal*, 216: 114776.